Difference in molecular mechanisms governing changes in membrane properties of phospholipid bilayers induced by addition of nonionic and zwitterionic surfactants

Yoshimichi Andoh[a,*], Sakiho Kitou[b], Susumu Okazaki[b,*]

[a] *Center for Computational Science, Graduate School of Engineering, Nagoya University, Furo-cho, Chikusa-ku, Nagoya 444-8604, Japan*
[b] *Department of Materials Chemistry, Nagoya University, Furo-cho, Chikusa-ku, Nagoya 444-8604, Japan*

Abstract

We investigated how nonionic surfactants (1-dodecanol, dodecyl methyl ester, and dodecanoic acid) and zwitterionic surfactants (*N*,*N*-dimethyldodecylamine *N*-oxide, and 1-lauroyl-2-hydroxy-*sn*-glycero-3-phosphatidylcholine) change the physicochemical properties of 1,2-dimyristoyl-*sn*-glycero-3-phosphocholine (DMPC) lipid bilayers in the liquid crystalline phase. The surfactants have a hydrophilic head group and hydrophobic saturated alkyl chain with 12 carbons long in common. A series of 100-ns-long all-atomistic molecular dynamics calculations were performed for fully hydrated binary lipid bilayers composed of DMPC and 33 mol% surfactant under isothermal–isobaric condition ($T = 303.15$ K, and $P = 1$ atm). All nonionic surfactants considered here induced structural ordering of DMPC lipid bilayers, as we reported in a previous paper on DMPC/ethylene-glycol-ether binary bilayers. In particular, the degree of the ordering was highest for dodecanoic acid, followed by

*Corresponding authors. Email : andoh@ccs.engg.nagoya-u.ac.jp (Y.A.), and okazaki@chembio.nagoya-u.ac.jp (S.O.)

1-dodecanol and dodecyl methyl ester. Both of the zwitterionic surfactants induced structural disordering of the DMPC lipid bilayers. We have clarified the different molecular mechanisms that govern changes in membrane properties induced by nonionic and zwitterionic surfactants.
Keywords: lipid bilayers, 1,2-dimyristoyl-*sn*-glycero-3-phosphocholine, nonionic and zwitterionic surfactants, molecular dynamics calculations, membrane properties

---

1. Introduction

Glycerophospholipid molecules dispersed in aqueous solution form lipid bilayers spontaneously [1, 2]. Lipid bilayers are the simplest model of biomembranes, such as cell plasma membranes. The physicochemical properties of lipid bilayers have been investigated experimentally and theoretically to understand the basic properties of biomembranes.

The physicochemical properties of single-component bilayers composed of glycerophospholipids, especially phosphatidylcholines (PCs), are altered by the addition of another type of lipid molecule. The best-known case is the structural ordering of PC bilayers in the liquid crystalline (L_α) phase upon the addition of cholesterol molecules. The ^{2}H-NMR measurements of the order parameter of the C-^{2}H bonds in the acyl tail, $S_{\rm CD}$, indicate that PC molecules in PC/cholesterol binary bilayers have more ordered acyl tails than in pure PC bilayers [3, 4, 5]. Further, with increasing amounts of cholesterol, up to several 10 mol%, the PC/cholesterol binary bilayers express another thermodynamic phase, referred to as the liquid-ordered ($L_{\rm o}$) phase [6, 7]. In the $L_{\rm o}$ phase, the bilayers are stiffer and have less membrane fluidity than pure PC bilayers. Existence of the $L_{\rm o}$ phase is the basis of discussion on the ordered microdomains in cell membranes (the lipid raft) [8]. Interestingly, ordering of phospholipid bilayers is also observed for mixed phospholipid bilayers with ceramides [9, 10], diacylglycerols [11], and straight-chain surfactants, such as ethylene glycol ethers with a small hydrophilic head group [12]. However, the molecular mechanism of the ordering could differ between these additive lipids.

In contrast, disordering of the PC bilayers in the L_α phase upon the ad-

dition of straight-chain surfactants with large hydrophilic head groups also occurs. The ^{2}H-NMR measurements of S_{CD} indicate that an incorporation of 33.3 mol% ethylene glycol ethers ($C_{12}E_8$) into 1,2-dimyristoyl-*sn*-glycero-3-phosphocholine (DMPC) bilayers induces lowering of the conformational ordering of the acyl tails [13, 14]. The ability of $C_{12}E_8$ to disorder the membrane structure of DMPC bilayers was also confirmed by our all-atomistic molecular dynamics (MD) calculations [12]. Further, we have also investigated, systematically, how changes in the size of the head group m and the length of tail n of C_nE_m molecules influence a direction of change in membrane properties by executing a series of all-atomistic MD calculations of DMPC/C_nE_m binary bilayers. We found that the trend of alteration strongly depends on both the size of the hydrophilic head group and the length of the hydrophobic tail. $C_{12}E_1$ and $C_{12}E_2$ induced the ordering of the DMPC bilayers, as does cholesterol. In contrast, $C_{12}E_4$, $C_{12}E_8$, and $C_{12}E_{10}$ induced the disordering of the DMPC bilayers. The molecular mechanisms have been clarified in detail [12, 15].

The aim of this research is to investigate whether straight-chain surfactant molecules with a small hydrophilic head group embedded in DMPC bilayers generally induce structural ordering of bilayers, or not, by performing all-atomistic MD calculations of DMPC/surfactant binary bilayers. The following surfactants were investigated: 1-dodecanol (named CDOH, here), dodecyl methyl ester (CDOM), and dodecanoic acid (CDAC) as typical nonionic surfactants, and *N*,*N*-dimethyldodecylamine *N*-oxide (DDAO) and 1-lauroyl-2-hydroxy-*sn*-glycero-3-phosphatidylcholine (LLPC) as typical zwitterionic surfactants. All have one hydrophilic head group and one hydropho-

bic saturated alkyl chain, with 12 carbons long in common. Carbon number 12 of surfactant alkyl chan is selected, because it enables us to compare the present MD results with our previous studies[12, 15] directly, as well as experimental studies on physical property changes in phospholipid/surfactant binary bilayers[16, 17, 18, 19, 20, 21, 22, 23, 24, 25] summarized in a review paper[26]. Results of MD calculations indicate that the nonionic surfactants considered here induced ordering of the membrane structure. The basic mechanism of the observed ordering is the same as that caused by $C_{12}E_m$ ($m \leq 2$) [12]. That is, the dodecyl tails of surfactant molecules fill voids inherent in the hydrophobic core of DMPC bilayers, enhancing the ordering of surrounding DMPC acyl tails. In contrast, the zwitterionic surfactants induce disordering of membrane structure. The zwitterionic head groups are deeply embedded within the water/bilayer interface, and then cause a steric hindrance against PC head groups of DMPC molecules crowded laterally at the interface. Such steric hindrance causes expansion of the membrane in the lateral direction, creating small voids beneath the head group. These voids permit the dodecyl tails of surfactant molecules, and surrounding acyl tails of DMPC molecules, to change their conformations more freely. Hence, the order of the hydrophobic core region is reduced in these binary bilayers. Our MD calculations have clarified that the membrane properties of DMPC bilayers are altered by nonionic and zwitterionic surfactants in different ways. We have also clarified a difference in molecular mechanisms according to which membrane properties are altered by nonionic and zwitterionic surfactants. This could not be discussed in detail by experimental studies[16, 17, 18, 19, 20, 21, 22, 23, 24, 25, 26].

2. Calculation

2.1. Molecular structure

The molecular structures of DMPC and surfactants are given in Fig. 1. DMPC has two saturated acyl tails, each 14 carbons long, and a PC head group, connected by a glycerol backbone. The nonionic surfactants CDOH, CDOM, and CDAC have one hydrophilic functional group and an alkyl chain, with 12 carbons long in common. Zwitterionic surfactants DDAO and LLPC have a zwitterionic head group and one alkyl chain, with 12 carbons long. AO and PC groups in DDAO and LLPC, respectively, have both positive and negative charges in them by protonation/deprotonation, though they are totally charge neutral as a group: i.e., zwitterions.

Under a neutral pH condition (pH=7.4) assumed here, there is a possibility that head groups of fatty acid are deprotonated, and a part of CDAC molecules become monovalent anionic lipids, since an acid dissociation constant pK_a for alkyl fatty acids are around 4.5 in a bulk aqueous solution. However, it is reported that the apparent pK_a value for fatty acids in monolayers or bilayers formed at an aqueous solution interface reaches over 9.0[27, 28]. So, all head groups of CDAC molecules are protonated in the present system. Further, it is confirmed experimentally that DDAO is charge-neutral in the physiological condition of pH[29].

2.2. Lipid bilayer system

A fully hydrated binary component lipid bilayer system was constructed as follows. The mole fraction of surfactants to the lipids was all 33 mol%, which is the same as used in our previous work [12]. First, 128 DMPC

molecules (64 per one leaflet) were arranged in a bilayer form. Then, 21 DMPC molecules of each leaflet were replaced by surfactant molecules with all-*trans* tail conformations. The position of the replacements was selected randomly. Second, the binary bilayer was sandwiched by water layers composed of 5120 water molecules in total. The number of water molecules per lipid n_{w} was 40, which is the same as in our previous work [12]. With this water amount, fully hydrated binary bilayers in the lamellar phase were obtained under three-dimensional (3D) periodic boundary conditions, as discussed in Section 3.2.

2.3. Molecular dynamics calculations

With regard to the force field, the all-atomistic CHARMM36 [30] and CHARMM General Force Field (CGenFF) [31] were adopted for lipids (DMPC and surfactants). The modified TIP3P (mTIP3P) [32] model was adopted for water. The Lennard-Jones interaction was cut off at 1.2 nm by applying the force switching function [33] from 0.8 nm to 1.2 nm. The Coulombic interaction was calculated by the particle mesh Ewald method [34]. The equation of motion was numerically solved by integrators based on the RESPA method [35, 36] with a time step of $\Delta t = 1$ fs, where distance constraints were introduced for all the chemical bonds relevant to hydrogen atoms. For water molecules, the H–H distance was also constrained for rigidifying the water molecule. These constraints were numerically solved by the SHAKE/RATTLE/ROLL algorithm [36, 37, 38].

First, the potential energy of an initial configuration of the calculation system was minimized by the steepest descent method. After assigning an initial temperature of 3.15 K, following the Maxwell–Boltzmann distribution

of velocities, the temperature was raised to 303.15 K, which is above the gel to liquid-crystalline phase transition temperature of pure DMPC bilayers (297 K [2]), in a stepwise fashion, using the velocity scaling method (ΔT = 50 K). After reaching 303.15 K, 100 ns (50 ns for equilibration, and 50 ns for analysis) MD calculations were carried out under isothermal isobaric conditions (T = 303.15 K, P = 1 atm). In production runs, the temperature was controlled by the Nose–Hoover chain method [39, 40]. The pressures normal to a bilayer (the z axis) and parallel to the bilayer (the x and y axes) were separately controlled by the Parrinello–Rahman method [41], as in the original CHARMM36 paper [30]. The membrane area, S, unit cell height, h, and unit cell volume, V, all converged to their equilibrium values within the first 50-ns MD calculations as shown in Figs. S1A and B in the Supplementary Material. Total potential energy, internal energy, and enthalpy of the system are also converged well as shown in Fig. S2A–C in the Supplementary Material. Equilibrated configurations of each system are shown in Fig. S3 in the Supplementary Material.

All MD calculations were carried out using the PME version of our originally developed software MODYLAS [42].

3. Results

3.1. Structural properties

Table 1 summarizes the structural properties of membranes averaged over the last 50 ns of MD calculations for each system. The properties of the pure DMPC bilayer under the same T and P conditions [12] as in the present study were taken from our previous paper (listed as a reference).

All three nonionic surfactants induced a decrease of S in the binary bilayers. The amount of decrease induced was in the order CDAC $\approx$ CDOM $>$ CDOH. The DMPC/zwitterionic surfactant bilayers also showed a slight decrease of S, although the degree of the reduction was much smaller than in the cases of the nonionic surfactants.

Membrane thickness h_l, which is defined as the difference between averaged z positions of phosphorus atoms in DMPC head groups in each monolayer, became greater in the order CDOM $>$ CDAC $>$ CDOH $>$ DDAO $>$ LLPC (see also Fig. S1C in the Supplementary Material, about convergence of h_l). h_l in the latter two cases is small if compared with h_l for a pure DMPC bilayer. This implies that the addition of DDAO and LLPC led to membrane disordering of these binary bilayers. The degree of order of membrane structure will be quantified directly by the order parameter of C–H vectors in DMPC acyl tails, as described below in Section 3.3.

In general, h_l is inversely proportional to S. The calculated values follow this general trend. One exception is h_l for the DMPC/CDOM bilayer, which has a similar S to the DMPC/CDAC bilayer. This may be because the distribution of CDOM molecules in the bilayer, whose head group ' s hydrophilicity is much weaker than head groups of other surfactant molecules,

differs greatly from the distributions of other surfactant molecules in the bilayer. Some of the CDOM molecules dissolve into the hydrophobic core of the bilayer, as will be discussed in Section 3.2. As a result, the membrane volume V_l, which is a product of S and h_l, becomes smaller in the order CDAC < CDOH < CDOM < DDAO < LLPC.

Further, the isothermal area compressibility, χ_T^S, and volume compressibility, χ_T^V, were calculated from the fluctuation of S and V. For example,

$$\chi_T^S = \frac{1}{k_{\mathrm{B}}T}\frac{\langle \delta S^2 \rangle}{\langle S \rangle} \tag{1}$$

where $\delta S^2 = (S - \langle S \rangle)^2$ and k_{B} is the Boltzmann constant. We calculated the fluctuation based on one 50-ns trajectory in an equilibrium state. The calculated χ_T^S values for DMPC/CDOH, DMPC/CDAC, DMPC/DDAO, and DMPC/LLPC binary bilayers become similar to those for pure DMPC bilayers, which indicates that these membranes are soft in the lateral direction, to the same degree as the DMPC bilayers in the L_α phase. The χ_T^S for the DMPC/CDOM bilayer becomes slightly larger than that for a pure DMPC bilayer, which indicates that the DMPC/CDOM bilayer becomes softer in the lateral direction. The calculated χ_T^V values for the DMPC/CDOH, DMPC/CDAC, DMPC/DDAO, and DMPC/LLPC binary bilayers are nearly equal to the value for the pure DMPC bilayer. This is because the compressibility of a fully hydrated bilayer system is determined by the compressibility of bulk water. The calculated χ_T^V for DMPC/CDOM bilayers is relatively large, mainly due to the large fluctuation of S.

Experimentally, it is reported that n-alcohols with chain lengths greater than 8 carbons incorporated into DMPC bilayers promote molecular packing in membranes[18]. Also, octanol and dodecanol incorporated into DMPC

bilayers raises the gel/liquid crystalline phase transition temperature of the DMPC bilayers[16, 17], which implies that packing of lipid molecules in these membranes is enhanced by addition of these n-alcohols. The observed smaller S and greater h_l in the DMPC/CDOH binary bilayer than the pure DMPC bilayer corresponds to these experimental results. It is verified that fatty acids with the similar number of carbon atoms as n-alcohols have the same effect on membrane properties[17, 20, 21]. This supports the observed smaller S and greater h_l in the DMPC/CDAC binary bilayer in the present study, too.

In contrast, thinning of phosphatidylcholine bilayers is observed by the neutron scattering or X-ray diffraction experiments[22, 23] where a series of alkyl dimethylamine oxides (ADAOs) is added to the bilayers. Especially, Dubnickova et. al. reported that 33.3 mol% of DDAO added to DMPC bilayers causes 15% reduction of bilayer thickness from pure DMPC bilayers at 309 K[22]. In the present calculation, reduction of h_l by 4% is also observed in the case of DMPC/DDAO bilayer . Difference in reduction rate between the experiment and present calculation is not important. It might be attributed to differences in mole fraction of DDAO, temperature condition, and definition of membrane thickness. Otherwise, an assumption by Dubnickova et. al. that the specific volume of lipid molecules are independent on their mixing ratio may cause some errors in their analysis.

Changes in membrane properties by incorporation of lysophospholipids is unclear from experimental measurements[24, 25]. It is explained only qualitatively that incorporated lysophospholipids into phospholipid bilayers cause disruptions to membrane structure. Relatively larger S and smaller h_l values

for the DMPC/LLPC bilayer may indicate structural disruption induced by LLPC. Within our knowledge, no experimental studies on membrane property changes for phospholipid/alkyl methyl esters binary bilayers are found. This may be because alkyl methyl esters with very low hydrophilicity of head group is out of interest as surfactants.

3.2. Number density profile along the bilayer normal

To investigate membrane structure in more detail, we calculated the number density profile of each segment, and representative atoms, along the bilayer normal, $\rho(z)$. Carbonyl oxygen atoms at the branch points of the *sn*-1 and *sn*-2 tails have an ability to form hydrogen bonds with surrounding molecules such as penetrated water molecules and surfactant head groups. It is therefore interesting to examine the z position of the hydrophilic head group of the surfactant molecule relative to the carbonyl groups of the DMPC molecule.

In the case of DMPC, nitrogen and phosphorus atoms in the PC head group, and each carbonyl group at the branch points of the acyl tails, were selected as a segment to calculate $\rho(z)$. For nonionic surfactants and DDAO, their hydrophilic head groups (OH, OM, AC, and DAO), and ethyl or methyl groups, with carbon numbers 4, 8, and 12, were adopted as the segment. For LLPC, nitrogen and phosphorus atoms in the PC head group, and carbonyl, ethyl, and methyl groups, with carbon numbers 4, 8, and 12, were adopted as the segment.

Figure 2 shows the calculated number density profile of representative segments and atoms $\rho(z)$ in phospholipid and surfactant molecules, and that of water molecule $\rho_{\mathrm{w}}(z)$. First, $\rho_{\mathrm{w}}(z)$ for all systems gives a plateau in the

water layer ($z \geq 3.0$ nm) between bilayers, which indicates that the binary bilayers are fully hydrated with a given n_{w}. The height of the plateaus of $\rho_{\mathrm{w}}(z)$ is identical for the five systems, as shown in Fig. S4 in the Supplementary Material.

In DMPC/nonionic surfactant bilayers, it is commonly observed that the peaks for hydrophilic head groups of surfactant molecules (OH, OM, and AC) locate at the inner side of the peaks for the carbonyl groups of DMPC molecules, where ' inner ' means closer to the bilayer center ($z = 0$). The relative arrangement of these peaks gives the molecular picture in which nonionic surfactant molecules hang on to the carbonyl groups by forming hydrogen bonds. One exception is the distribution of the OM head group. $\rho(z)$ for OM head groups has one more peak centered at $z = 0$. Because the hydrophilicity of the OM head group is rather weak (among the surfactant head groups considered here), some CDOM molecules are dissolved into the hydrophobic core of the bilayer as a result of thermal fluctuation along the z axis (see Fig. S5 in the Supplementary Material). An anomalous increase of h_l in the DMPC/CDOM bilayer (as mentioned in the previous section) can be attributed to these dissolved CDOM molecules: some of them are located at the bilayer center, which should thicken the hydrophobic core region.

Further, it is interesting to find that, in DMPC/DDAO bilayers, the peak for zwitterionic DAO head groups of DDAO molecules is located between the peaks for carbonyl groups and phosphorus atoms in the PC head group of DMPC molecules, as shown in Fig. 2D. This means that, unlike OH, OM, and AC head groups, zwitterionic DAO head groups are deeply embedded within the interfacial region between water and bilayer, where PC

head groups of DMPC molecules are crowded laterally, being sandwiched by phosphate groups and carbonyl groups of DMPC molecules. A schematic of the different positions of CDOH and DDAO molecules in binary bilayers is shown in Fig. S5 in the Supplementary Material.

In DMPC/LLPC bilayers, PC head groups of LLPC molecules are also deeply embedded within the interfacial region as shown in Fig. 2E. The peak positions of nitrogen and phosphorus atoms, and the carbonyl group, shift slightly toward the water phase, perhaps because of the lack of a bulky *sn*-2 chain. Furthermore, these peaks are wider than the peaks of the nitrogen and phosphorus atoms in the PC head group of the DMPC molecule. The reason for this may be a shortage of statistics. (Note that numbers of molecules are 43 and 21 for DMPC and LLPC, respectively.)

For every binary bilayer case, peak positions of $\rho(z)$ for ethyl and methyl segments in the dodecyl tail of surfactant molecules are located in the order from segments with a low number of carbons to those with a high number of carbons toward the bilayer center. Further, the peak height of $\rho(z)$ for the C4 ethyl group is equivalent to that for the C8 ethyl group, which indicates that the hydrophobic tails of surfactants are arranged in parallel to the bilayer normal, with the head group trapped at the water/bilayer interface. For the DMPC/CDOM bilayer, however, the peak heights of $\rho(z)$ for the C4 and C8 ethyl groups are not equivalent. This is because some of the CDOM molecules are dissolved into the hydrophobic core of the bilayer.

The peak of $\rho(z)$ for the terminal C12 methyl group of the DDAO tail is found furthest from the bilayer center among other C12 methyl groups, as shown in Fig. 2D. We believe that this is caused by strong anchoring

of zwitterionic head groups of DDAO molecules to the interface, shifting the molecule ' s position closer to the water layer (see also Fig. S5 in the Supplementary Material).

3.3. Order parameter of the C–H vector

The degree of order of the acyl tails of DMPC molecules and dodecyl tail of surfactant molecules can be measured by the order parameter of the C–H vectors in these tails, S_{CH}, which is defined by

$$S_{\mathrm{CH}} = \left| \left\langle \frac{1}{2} \left(3\cos^2\theta - 1 \right) \right\rangle \right| \tag{2}$$

where θ is the angle between the C–H vector and the bilayer normal, and $\langle ... \rangle$ indicates the ensemble average. The higher the S_{CH} value is, the more the conformation of the tail is ordered.

Figure 3 shows the calculated S_{CH} in the *sn*-1 and *sn*-2 acyl tails of the DMPC molecule (panels A and B, respectively), and dodecyl tails of surfactant molecules (panel C), as a function of the carbon number in each tail. As is commonly observed in binary bilayers with nonionic surfactants, the acyl tails of DMPC molecules are more ordered than those of the pure DMPC bilayers. The degree of order is as follows: CDAC > CDOH > CDOM. In contrast, in binary bilayers with zwitterionic surfactants, S_{CH} is lower than S_{CH} for pure DMPC bilayers. Unexpectedly, the order is quite low in the DMPC/LLPC bilayer.

With regard to the dodecyl tail of the surfactant, the degree of order is high for CDOH and CDAC molecules, and similar to that of the acyl tails of DMPC molecules, which constitute the binary bilayer. For the other three surfactants, the direction of change in S_{CH} is not straightforward. The

calculated S_{CH} value for the CDOM dodecyl tail is much lower than that for the CDOH and CDAC dodecyl tails, although DMPC acyl tails in the DMPC/CDOM bilayer retain high order, comparable with in DMPC/CDOH and DMPC/CDAC bilayers. Lowering of the S_{CH} value for the CDOM dodecyl tail results from the fact that some CDOM molecules are dissolved into the hydrophobic core region, with irregular orientation to the bilayer normal. For DDAO and LLPC dodecyl tails, the calculated S_{CH} value of carbon number 2 becomes highest, followed by a monotonical decrease toward the chain end. The highest S_{CH} at the root of these dodecyl tails will be attributed to strong anchoring of the hydrophilic head groups of these zwitterionic surfactant molecules to the water/bilayer interface.

4. Discussion

To clarify the molecular mechanism of change in membrane properties (observed as described in the Results section), we carried out further analyses.

4.1. Two-dimensional radius of gyration of lipid molecules

The radius of gyration of lipid molecules projected on the x–y plane $R_{\mathrm{g}}^{\mathrm{2D}}$ was calculated. $R_{\mathrm{g}}^{\mathrm{2D}}$ provides useful information to understand why the mixed bilayers shrunk or extended laterally. In addition to $R_{\mathrm{g}}^{\mathrm{2D}}$ for the whole molecule, $R_{\mathrm{g}}^{\mathrm{2D}}$ for the hydrophilic head group and hydrophobic tail(s) of lipid molecules was separately calculated.

$R_{\mathrm{g}}^{\mathrm{2D}}$ is calculated as follows:

$$R_{\mathrm{g}}^{\mathrm{2D}} = \sqrt{\left\langle \frac{\sum_{i=1}^{N} (\boldsymbol{r}_i - \boldsymbol{R})^2}{N} \right\rangle} \tag{3}$$

where $\boldsymbol{r}_i$ is the coordinate of the ith atom, $\boldsymbol{R}$ is the center of mass of the whole molecule or segment, and N is the number of atoms that constitute the whole molecule or segment. Only the x, y components of $\boldsymbol{r}_i$ and $\boldsymbol{R}$ were used in the calculation.

Table 2 lists the calculated $R_{\mathrm{g}}^{\mathrm{2D}}$ values. In DMPC/nonionic surfactant binary bilayers, the $R_{\mathrm{g}}^{\mathrm{2D}}$ value for the whole DMPC molecule becomes smaller than that in a pure DMPC bilayer. The $R_{\mathrm{g}}^{\mathrm{2D}}$ value for the two acyl tails is also smaller in these binary bilayers because the two acyl tails are ordered in these binary bilayers, as shown in Figs. 3A and 3B. Thus, a smaller $R_{\mathrm{g}}^{\mathrm{2D}}$ value for the whole DMPC molecule results from more ordered acyl tails in these binary bilayers than in a pure DMPC bilayer.

R_g^{2D} values for the whole CDOH and CDAC molecules are also smaller than the R_g^{2D} value for the whole DMPC molecule. This is because the sectional area of a surfactant molecule with one straight chain is generally small. As a result, S for DMPC/CDOH and DMPC/CDAC bilayers becomes smaller than for a pure DMPC bilayer. The rather large value of R_g^{2D} for the whole CDOM molecule is due to the fact that some CDOM molecules are dissolved into the hydrophobic core of the bilayer with a laterally spread conformation. However, only CDOM molecules aligned parallel to the z axis having a small sectional area contribute to S. Therefore, DMPC/CDOM bilayers also have smaller S than pure DMPC bilayers.

In DMPC/zwitterionic surfactant binary bilayers, R_g^{2D} values for the whole DMPC molecule become similar to, or slightly larger than, values for pure DMPC bilayers. A much larger R_g^{2D} value for the whole DMPC molecule in the DMPC/LLPC bilayer is attributed to large R_g^{2D} values for the two acyl tails of the DMPC molecule. They have the most disordered conformation among the five systems, as shown in Figs. 3A and 3B.

R_g^{2D} values for whole DDAO and LLPC molecules become larger than values for nonionic surfactants, but they are still smaller than that for the whole DMPC molecule. As expected from its molecular structure, R_g^{2D} values for their zwitterionic head groups (DAO and PC) become larger than for nonionic surfactant head groups (OH, OM, and AC). In particular, the R_g^{2D} value for the PC head group of the LLPC molecule is comparable with the R_g^{2D} value for the PC head group of the DMPC molecule. Furthermore, the R_g^{2D} value for the dodecyl tail of the LLPC molecule is largest among all surfactants, which is attributed to the dodecyl tail of LLPC being the

most disordered, as shown in Fig. 3C. Hence, DMPC/zwitterionic surfactant binary bilayers give relatively larger S value than DMPC/nonionic surfactant bilayers.

Moreover, we found that the position of zwitterionic head groups relative to DMPC carbonyl groups along the bilayer normal also contributes to relatively large S values in DMPC/zwitterionic surfactant binary bilayers. As shown in Figs. 2D and 2E, zwitterionic DAO and PC head groups of DDAO and LLPC molecules are deeply embedded within the water/bilayer interface. Thus, the two-dimensional (2D) size of zwitterionic head groups, which is proportional to $(R_{\mathrm{g}}^{\mathrm{2D}})^2$, contributes directly to an increase of S, by pushing surrounding PC head groups and the backbone motif of DMPC molecules laterally, with a steric hindrance. In contrast, such an effect will be small for nonionic surfactants because their head groups are buried at the inner side of carbonyl groups of DMPC molecules.

4.2. Lateral radial distribution function of lipid molecule centers of mass

The lateral packing of centers of mass of DMPC and surfactant molecules in bilayers was investigated using a 2D lateral distribution function between centers of mass of lipid molecules, $g_{ij}^{\mathrm{2D}}(r)$. It is defined by

$$g_{ij}^{\mathrm{2D}}(r) = \frac{\langle H_{ij}(r) \rangle}{2\pi r \Delta r \langle \rho_j \rangle} \tag{4}$$

where r is a lateral distance between the centers of mass of ith and jth types of molecules, $\langle H_{ij}(r) \rangle$ is the averaged number of the jth type of lipid molecules around the ith type of lipid molecule whose distance is between $r - \frac{\Delta r}{2}$ and $r + \frac{\Delta r}{2}$, and ρ_j is a 2D number density of the jth type of lipid molecule.

The function was calculated independently for pairs between DMPC–DMPC molecules, DMPC–surfactant molecules, and surfactant–surfactant molecules.

Figure 4 shows the calculated functions for DMPC–DMPC molecules, $g^{\mathrm{2D}}_{\mathrm{DMPC-DMPC}}(r)$ (panel A), for DMPC–surfactant molecules, $g^{\mathrm{2D}}_{\mathrm{DMPC-surfact.}}(r)$ (panel B), and for surfactant–surfactant molecules, $g^{\mathrm{2D}}_{\mathrm{surfact.-surfact.}}(r)$ (panel C).

In Fig. 4A, positions of the first peaks of $g^{\mathrm{2D}}_{\mathrm{DMPC-DMPC}}(r)$ for DMPC/nonionic surfactant binary bilayers correspond to those in the pure DMPC bilayer. This means that the positional correlation between the centers of mass of DMPC molecules is not greatly affected by the addition of 33 mol% nonionic surfactant into the bilayer. The heights of the first peaks of $g^{\mathrm{2D}}_{\mathrm{DMPC-DMPC}}(r)$ for the DMPC/CDAC binary bilayer is higher than the others, which indicates that the lateral arrangement of DMPC molecules is ordered by embedded CDAC molecules.

In contrast, the heights of the first peaks of $g^{\mathrm{2D}}_{\mathrm{DMPC-DMPC}}(r)$ for the DMPC/zwitterionic surfactant binary bilayers are noticeably lower. These lower peak heights indicate that the lateral arrangement of DMPC molecules is disturbed by embedded zwitterionic surfactant molecules. This is because zwiterionic head groups of DDAO and LLPC molecules are embedded deeply within the water/bilayer interface, as shown in Figs. 2D and 2E. These embedded head groups should disturb the lateral arrangement of DMPC molecules, causing lowering of the height of the first peak of $g^{\mathrm{2D}}_{\mathrm{DMPC-DMPC}}(r)$ in these bilayers.

In Fig. 4B, it is apparent that the positions of the first peaks of $g^{\mathrm{2D}}_{\mathrm{DMPC-CDOH}}(r)$, $g^{\mathrm{2D}}_{\mathrm{DMPC-CDAC}}(r)$, and $g^{\mathrm{2D}}_{\mathrm{DMPC-DDAO}}(r)$ are shifted further to the inner side

of the first peak of $g^{2D}_{DMPC-DMPC}(r)$ in pure DMPC bilayers. This indicates that CDOH, CDAC, and DDAO molecules are packed more closely around the centered DMPC molecule than other DMPC molecules in these DMPC/surfactant binary bilayers. For DMPC/CDOH and DMPC/CDAC binary bilayers, hydrocarbon tails of these closely packed surfactant molecules may fill voids between the acyl tails of DMPC molecules existing in a pure DMPC bilayer, as we discussed in our previous study [12], and then make these acyl tails more ordered in binary bilayers. For DMPC/DDAO binary bilayers, a steric hindrance of DDAO head groups, which are deeply embedded within the water/bilayer interface, may prevent the tails from closer packing. The number of voids in a membrane is quantified in the next section.

The position of the first peak of $g^{2D}_{DMPC-LLPC}(r)$ is nearly the same as that of $g^{2D}_{DMPC-DMPC}(r)$. Taking into account that LLPC molecules have only one tail, it is expected that many voids may be created at the inner side of their glycerol backbone. Due to these additional voids (the detection of which is described in the next section), the dodecyl tails and the acyl tails of surrounding DMPC molecules will have disordered conformation. Indeed, the calculated S_{CH} becomes quite low for both dodecyl and acyl tails, as shown in Figs. 3A–3C. For $g^{2D}_{DMPC-CDOM}(r)$, no clear first peak is observed because some CDOM is dissolved into the hydrophobic core region of the bilayer, with its very weak hydrophilicity at the OM head group, as discussed above.

In Fig. 4C, very clear oscillatory behavior is observed for $g^{2D}_{CDOH-CDOH}(r)$ and $g^{2D}_{CDAC-CDAC}(r)$ continuing up to 2.0 nm, which means that lateral arrangements of CDOH and CDAC molecules are strongly correlated in these binary bilayers. $g^{2D}_{CDOM-CDOM}(r)$ and $g^{2D}_{DDAO-DDAO}(r)$ also show oscillatory

behavior, although their amplitude is smaller than the former two cases. Further, $g^{\mathrm{2D}}_{\mathrm{LLPC-LLPC}}(r)$ has only one shallow first peak, followed by a wide well, indicating that there is no clear correlation between LLPC molecules in the bilayer, perhaps because its molecular structure is very similar to that of DMPC.

4.3. Void distribution in membranes

To support the discussion in the previous section, we detected voids in membranes and calculated a probability distribution of voids along the z axis, $P_{\mathrm{void}}(z)$, using the same method as we reported previously [12]. First, a hypothetical 3D mesh with a distance between knots of 0.1 nm was submerged into the calculation system. If a knot does not touch any atoms of lipid and water molecules, which have a van der Waals radius of σ ($\sigma = A/2^{1/6}$ where A is the Lennard-Jones parameter of the atom defined by the force field), it is regarded as a knot in voids. Then, $P_{\mathrm{void}}(z)$ was calculated as the ratio of the number of the knots in voids to the number of all knots at z, taking a time average of them.

Figure 5 shows the calculated $P_{\mathrm{void}}(z)$. For ordered DMPC/CDOH and DMPC/CDAC bilayers, $P_{\mathrm{void}}(z)$ at the middle of each leaflet (0.4 nm $\leq z \leq$ 1.0 nm) becomes smaller than that for pure DMPC bilayers. This supports a molecular picture in which acyl tails of DMPC molecules and dodecyl tails of surfactant molecules in the binary bilayers are more closely packed in the lateral direction than in pure DMPC bilayers. The tails with a small number of voids in their surroundings are forced to be ordered. Aagaard et al.[18] measured changes in molar volume of transfer ΔV of n-alcohols from the pure liquid state to DMPC bilayer, and found that CDOH shows

large negative value of ΔV. An origin of the negative ΔV was attributed to promoted molecular packing in the hydrophobic core region of the bilayer where the free volume is occupied by CDOH alkyl chains. Smaller $P_{\rm void}(z)$ for DMPC/CDOH bilayer than pure DMPC bilayer qualitatively agrees well with their inference.

For DMPC/CDOM bilayers, the shape of $P_{\rm void}(z)$ is somewhat misleading. We note that the position of the minimum of $P_{\rm void}(z)$ for the DMPC/CDOM bilayer (shown by an upward small black arrow in the figure) is shifted toward the water layer, because the membrane becomes thicker than pure DMPC bilayers. Therefore, if we scale $P_{\rm void}(z)$ for the DMPC/CDOM bilayer to match the position of its minimum to that for the pure DMPC bilayer (upward small gray arrow), keeping its shape, it is clear that voids at the middle of each leaflet in DMPC/CDOM bilayers also decrease. For scaled $P_{\rm void}(z)$, see also Fig. S6 in the Supplementary Material.

In contrast, for a disordered DMPC/LLPC bilayer, $P_{\rm void}(z)$ at the middle of each leaflet becomes larger than for a pure DMPC bilayer. These voids will be created by a steric hindrance of the bulky backbone of LLPC molecules against surrounding DMPC molecules, with their hydrophilic PC head group being deeply embedded within the water/bilayer interface, as discussed above. The tails, with a large number of voids in their surroundings, are forced to be disordered. These additional voids produced by incorporated LLPC molecules could cause disruptions of membrane structure observed in the experimental studies[24, 25, 26].

For DMPC/DDAO bilayers, by applying the same scaling to $P_{\rm void}(z)$ as in the DMPC/CDOM bilayer case, we find a small but evident increase of

voids at the middle of each leaflet compared with pure DMPC bilayers (see also Fig. S6 in the Supplementary Material). Because their DAO head groups are embedded in the interfacial region, additional voids are also created by a steric hindrance against surrounding DMPC molecules. However, DDAO molecules do not have a bulky backbone like LLPC; hence, the number of voids created in the DMPC/DDAO bilayer becomes smaller than in the DMPC/LLPC bilayer. The less disordering of acyl tails of DMPC molecules in the DMPC/DDAO bilayer than in the DMPC/LLPC bilayer results from fewer additional voids in the former bilayer.

4.4. Possibility of phase separation

A phase diagram suggested on the basis of experimental measurement[16, 21] indicates that fully-hydrated DMPC/CDOH and DMPC/CDAC bilayers with 33 mol% of surfactants may be within the coexisting region of the liquid crystalline and gel phases at 303.15 K. There is a possibility that DMPC/CDOH and DMPC/CDAC bilayers in the present calculation exhibit the lateral phase separation with longer simulation time, if we prepare larger bilayers in a lateral direction. In general, however, exact reproduction of the gel to liquid crystalline phase transition temperature is difficult by MD calculations even for one-component bulk solutions. So, we limited our discussions here only to fundamental changes caused by addition of these surfactant molecules.

On the other hand, it is reported that binary DMPC/DDAO binary bilayers are in the liquid crystalline phase up to at least 33 mol% of surfactant around 310.15 K[22], while DMPC/lyso-myristic-PC binary bilayers do not show the gel to liquid crystalline phase transition up to 50 mol% concentra-

tion of the lyso-PC at 303.15 K[24]. So, we infer that DMPC/DDAO and DMPC/LLPC bilayers in the present calculation may not exhibit the lateral phase separation even in longer simulation time. Instead of this, formations of small domains by concentration fluctuation of DDAO or LLPC could occur because of the hydrophobic mismatch[2] between DMPC and these surfactant molecules.

Within our knowledge, there are no experimental studies on the phase behavior of DMPC/alkyl-methyl-ester binary bilayers. Our simulation results (Fig. 2B, and Fig. S3) show that some CDOM molecules are dissolved into the hydrophobic core of the bilayer because of the weak hydrophilicity of the OM head group. Such incorporated CDOM molecules should cause unstablization of the bilayer. So it is expected that the DMPC/CDOM bilayer in the present calculation will show a macroscopic phase transition from the lamellar phase to the non-lamellar phases, if longer-time MD simulations are performed for larger calculation system.

5. Conclusion

We carried out 100-ns-long all-atomistic MD dynamics calculations for fully hydrated binary bilayers composed of DMPC and three types of nonionic surfactants (CDOH, CDOM, and CDAC), and two types of zwitterionic surfactants (DDAO and LLPC), under isothermal isobaric conditions (T = 303.15 K, P = 1 atm). Changes in membrane properties of DMPC bilayers, induced by addition of these surfactants (33 mol%), and the associated molecular mechanisms were investigated in detail. The three nonionic surfactants induced lateral shrinking of binary bilayers, with structural ordering of DMPC acyl tails. Here, CDAC has the highest ability to induce the ordering, followed by CDOH and CDOM. Interestingly, CDOM, whose head group ' s hydrophilicity is very weak, partly dissolves into the hydrophobic core region, but retains an ability to promote ordering of surrounding DMPC acyl tails. The mechanism of the ordering observed here is basically the same as that observed in DMPC/ $C_{12}E_m$ ($m \leq 2$) binary bilayers [12]. That is, small hydrophilic head groups of these surfactant molecules are buried at the inner side of the acyl tails of DMPC molecules, with their dodecyl tail sticking out toward the bilayer center. Voids inherent in pure DMPC bilayers are filled by the dodecyl tails. Ordering of the surrounding DMPC acyl tails is then enhanced. In contrast, two zwitterionic surfactants induced disordering of membrane structure. Further, LLPC caused greater disordering than DDAO. The following mechanism may apply here. Zwitterionic head groups are deeply embedded within the water/bilayer interface, where PC head groups of DMPC molecules are laterally crowded. The zwitterionic head group causes a steric hindrance against the surrounding PC head groups

and glycerol backbone, which enables the bilayer to expand in a lateral direction. Additional voids created in the hydrophobic core region of bilayers permit the acyl tails of surrounding DMPC molecules to change their conformations more freely. As a result, the degree of order of the acyl tails in these binary bilayers is reduced. The difference in molecular mechanisms by which membrane properties are altered by nonionic and zwitterionic surfactants arises from small differences in the chemical structures of the respective surfactants ' head groups.

In experiments on biomembranes, such as plasma membranes of cells, many different types of fluorescent surfactants are used to measure membrane properties. However, our results indicate that physicochemical properties of biological membranes are highly sensitive to the chemical structure of embedded surfactant molecules. Thus, the experimentally observed results should be discussed carefully. The membrane properties may also be sensitive to the chemical modification of lipid head groups and other additives adsorbed to the water/membrane interface.

Acknowledgements

This research was supported by MEXT as "Priority Issue on Post-K computer" (Development of new fundamental technologies for high-efficiency energy creation, conversion/storage and use), using computational resources of the K computer provided by the RIKEN Advanced Institute for Computational Science through the HPCI System Research project (Proposal number: hp170241). Calculations were mainly performed at the Information Technology Center (ITC) of Nagoya University, at the Institute for Solid State Physics, the University of Tokyo, and partially at the Research Center for Computational Science, Okazaki, Japan. This work is partly supported by "Joint Usage/Research Center for Interdisciplinary Large-Scale Information Infrastructures" in Japan (Proposal number: jh170024). This work is also supported by JSPS KAKENHI Grant Number 16K21094 (Y.A.).

References

[1] D. Voet, J. G. Voet, Biochemistry, fourth ed., Wiley-Interscience, New York, 2011.

[2] M. Luckey, Membrane Structural Biology: with Biological Biophysical Foundations, second ed., Cambridge University Press, New York, 2014.

[3] G. W. Stockton, C. F. Polnaszek, L. C. Leitch, A. P. Tulloch, I. C. P. Smith, Biochem. Biophys. Res. Commun. 60 (1974) 844.

[4] G. W. Stockton, I. C. P. Smith, Chem. Phys. Lipids 17 (1976) 251.

[5] M. Jansson, R. L. Thurmond, J. A. Barry, and M. F. Brown, J. Phys. Chem. 96 (1992) 9532.

[6] M. R. Vist, and J. H. Davis, Biochemistry 29 (1990) 451.

[7] D. Marsh, Biochim. Biophys. Acta 1798 (2010) 688.

[8] D. Lingwood, K. Simons, Science 327 (2010) 46.

[9] S. A. Pandit, S. W. Chiu, E. Jakobsson, et al. Biophys. J. 92 (2007) 920.

[10] E. Wang, J. B. Klauda, J. Phys. Chem. B 121 (2017) 10091.

[11] M. Alwarawrah, J. Dai, J. Huang, J. Chem. Theory Comput. 8 (2012) 749.

[12] Y. Andoh, S. N. S. Mohamed, S. Kitou, S. Okazaki, Mol. Siml. 43 (2017) 1247.

[13] R. L. Thurmond, D. Otten, M. F. Brown, K. Beyer, J. Phys. Chem. 98 (1994) 972.

[14] D. Otten, M. F. Brown, K. Beyer, J. Phys. Chem. B 104 (2000) 12119.

[15] Y. Andoh, S. Muraoka, S. Okazaki, Mol. Siml. 41 (2015) 955.

[16] A. G. Lee, Biochemistry, 15 (1976) 2448.

[17] A. W. Eliasz, D. Chapman, D. F. Ewing, Biochim. Biophys. Acta, 448 (1976) 220.

[18] T. H. Aagaard, M. N. Kristensen, P. Wesh, Biophys. Chem., 119 (2006) 61.

[19] P. W. Westerman, J. M. Pope, N. Phonphok, J. W. Doane, D. W. Dubro, Biochim. Biophys. Acta, 939 (1988) 64.

[20] S. E. Schullery, T. A. Seder, D. A. Weinstein, D. A. Bryant, Biochemistry, 20 (1981) 6818.

[21] H. L. Kantor, J. H. Prestegard, Biochemistry, 17 (1978) 3592.

[22] M. Dubnickova, M. Kiselev, S. Kutuzov, F. Devinsky, V. Gordeliy, P. Balgavy, Gen. Physiol. Biophys, 16 (1997) 175.

[23] J. Karlovska, K. Lohner, G. Degovics, I. Lacko, F. Devinsky, P. Balgavy, Chem. Phys. Lipid, 129 (2004) 31.

[24] W. E. Klopfenstein, B. de Kruyff, A. J. Verkleij, R. A. Demel, L. L. M. van Deene, Chem. Phys. Lipids, 13 (1974) 215.

[25] G. J. A. van Echteld, B. de Kruijff, J. de Gier, Biochim. Biophys. Acta, 595 (1980) 71.

[26] A. G. Lee, Biochim. Biophys. Acta, 472 (1977) 285.

[27] H. Hauser, A. Darke, M. C. Phillips, Eur. J. Biochim., 62 (1976) 335.

[28] J. R. Kanicky, D. O. Shah, J. Colloid Interf. Sci., 256 (2002) 201.

[29] K. W. Herrman, J. Phys. Chem., 68 (1964) 1540.

[30] J. B. Klauda, R. M. Venable, J. A. Freites, J. W. O'Connor, D. J. Tobias, C. M. Ramirez, I. Vorobyov, A. D. MacKerell Jr, R. W. Pastor, J. Phys. Chem. B. 114 (2010) 7830.

[31] K. Vanommeslaeghe, E. Hatcher, C. Acharya, S. Kundu, S. Zhong, J. Shim, E. Darian, O. Guvench, P. Lopes, I. Vorobyov, A. D. Mackerell Jr, J. Comput. Chem. 31 (2010) 671.

[32] S. R. Durell, B. R. Brooks, A. Ben-Naim, J. Phys. Chem. 98 (1994) 2198.

[33] P. J. Steinbach, B. R. Brooks, J. Comput. Chem. 15 (1994) 667.

[34] U. Essmann, L. Perera, M. L. Berkowitz, T. Darden, H. Lee, L. G. Pedersen, J. Chem. Phys. 103 (1995) 8577.

[35] M. Tuckerman, B. J. Berne, J. Chem. Phys. 97 (1992) 1990.

[36] G. J. Martyna, M. E. Tuckerman, D. J. Tobias, M. L. Klein, Mol. Phys. 87 (1996) 1117.

[37] J.P. Ryckaert, G. Ciccotti, H. J. C. Berendsen, J. Comput. Phys. 23 (1977) 327.

[38] H.C. Andersen, J. Comput. Phys. 52 (1983), 24.

[39] S. Nosé, Mol. Phys. 52 (1984) 255.

[40] G. J. Martyna, M. E. Tuckerman, M. L. Klein, J. Chem. Phys. 97 (1992) 1990.

[41] M. Parrinello, A. Rahman, Phys. Rev. Lett. 45 (1980) 1196.

[42] Y. Andoh, N. Yoshii, K. Fujimoto, K. Mizutani, H. Kojima, A. Yamada, S. Okazaki, K. Kawaguchi, H. Nagao, K. Iwahashi, F. Mizutani, K. Minami, S. Ichikawa, H. Komatsu, S. Ishizuki, Y. Takeda, M. Fukushima, J. Chem. Theor. Comput. 9 (2013) 3201.

Tables

Table 1: Calculated structural and thermodynamic properties of DMPC/surfactant binary bilayers averaged over the last 50 ns. The values for the pure DMPC bilayer are taken from our previous paper [12]. Errors in the first six quantities are defined as the standard deviation values among five 10-ns interval averages. Errors in the last two quantities represent a propagated error of the standard deviation of the variance $\langle \delta S^2 \rangle$ or $\langle \delta V^2 \rangle$ and the error in $\langle S \rangle$ or $\langle V \rangle$.

	DMPC/surfactants					pure DMPC [12]
	CDOH	CDOM	CDAC	DDAO	LLPC	
$S(\mathrm{nm}^2)$	29.0±0.3	28.7±0.6	28.7±0.2	33.3±0.3	37.3±0.2	39.5±0.3
$A(\mathrm{nm}^2)$	0.453±0.005	0.449±0.009	0.448±0.003	0.520±0.005	0.583±0.004	0.617±0.005
$h_l(\mathrm{nm})$	3.82±0.03	3.94±0.05	3.86±0.02	3.42±0.03	3.18±0.03	3.55±0.03
$h(\mathrm{nm})$	9.03±0.09	9.19±0.17	9.13±0.07	7.92±0.07	7.34±0.05	7.40±0.06
$V_l(\mathrm{nm}^3)$	110.6±0.4	112.9±0.8	110.5±0.2	113.8±0.3	118.6±0.7	140.2±0.2
$V(\mathrm{nm}^3)$	261.7±0.1	263.5±0.3	261.7±0.1	263.8±0.6	273.6±0.1	292.2±0.1
$\chi_T^S(\mathrm{m}^2\mathrm{J}^{-1})$	3.9±0.2	6.1±0.5	3.6±0.1	4.2±0.2	3.6±0.1	4.4±0.1
$\chi_T^V(10^{-9}\ \mathrm{Pa}^{-1})$	0.70±0.01	0.83±0.01	0.71±0.01	0.66±0.01	0.64±0.01	0.67±0.01

Table 2: The calculated R_g^{2D} for the whole molecule and segments in DMPC and surfactant molecules. Two types of segments are considered: hydrophilic head groups and hydrophobic tail(s). The unit for all values in this table is nm. The values for a pure DMPC bilayer are taken from our previous paper [12]. The errors are the standard deviation values among five 10-ns interval averages.

system	DMPC/surfactants					pure DMPC [12]
	CDOH	CDOM	CDAC	DDAO	LLPC	
DMPC						
whole molecule	0.430±0.006	0.435±0.008	0.423±0.002	0.474±0.007	0.508±0.006	0.473±0.004
head group	0.240±0.001	0.241±0.001	0.240±0.001	0.235±0.001	0.241±0.001	0.240±0.001
two tails	0.428±0.007	0.435±0.009	0.416±0.004	0.487±0.011	0.527±0.011	0.486±0.007
Surfactants						
whole molecule	0.232±0.003	0.722±0.004	0.242±0.003	0.277±0.002	0.384±0.003	–
head group	0.057±0.001	0.099±0.001	0.095±0.001	0.158±0.001	0.241±0.001	–
tail	0.226±0.003	0.749±0.004	0.223±0.003	0.244±0.002	0.343±0.004	–

Figures

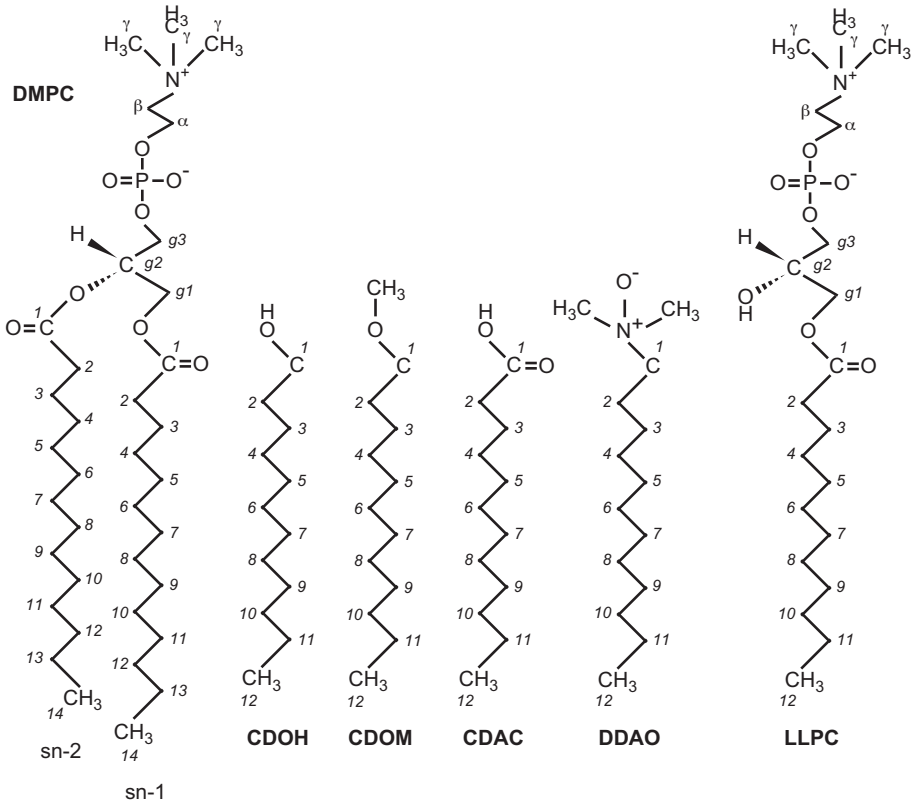

Figure 1: Molecular structure of DMPC and surfactant molecules, 1-dodecanol (CDOH), dodecanoic acid (CDAC), dodecyl methyl ester (CDOM), *N*,*N*-dimethyldodecylamine *N*-oxide (DDAO), and 1-lauroyl-2-hydroxy-*sn*-glycero-3-phosphatidylcholine (LLPC). Numbers in italic font in the figure indicate the numbers of carbons (noted in the main text).

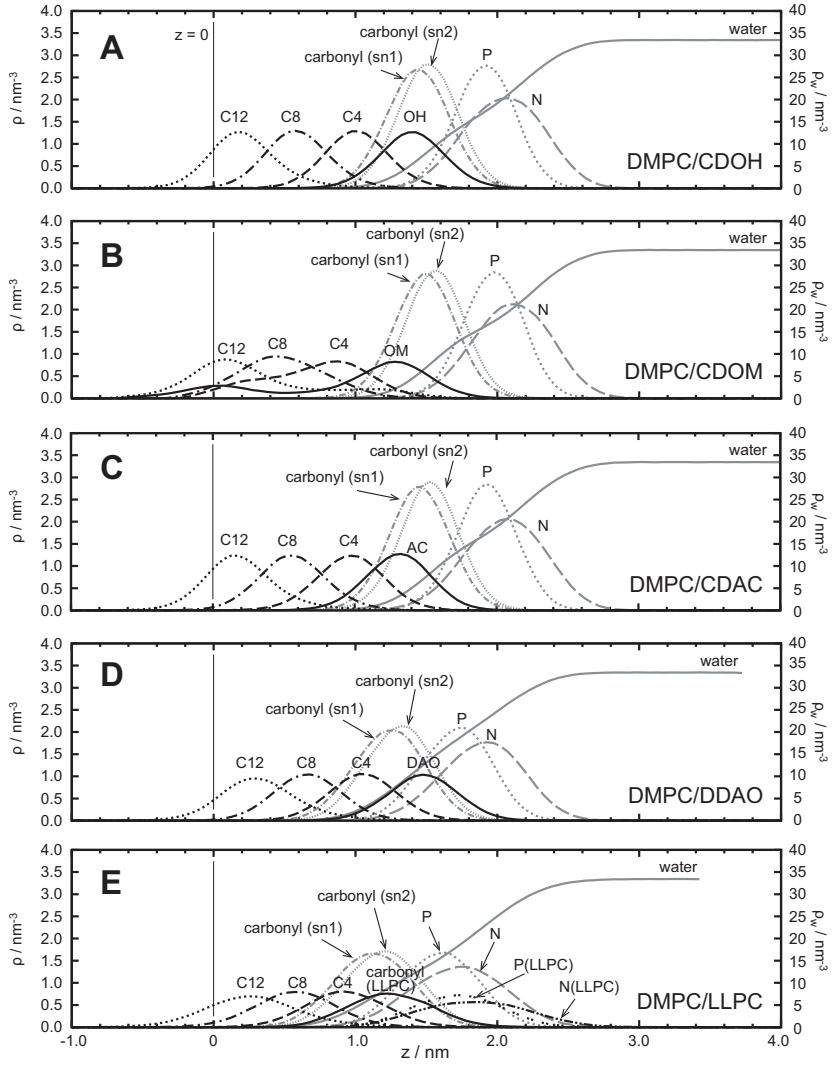

Figure 2: The calculated $\rho(z)$ and $\rho_{\rm w}(z)$ for binary bilayers: DMPC/CDOH (panel A), DMPC/CDOM (panel B), DMPC/CDAC (panel C), DMPC/DDAO (panel D), and DMPC/LLPC (panel E). $\rho(z)$ values are calculated for lipid molecules in each leaflet, then averaged over two leaflets. The origin of z corresponds to the center of mass of the binary bilayer. Gray lines are $\rho(z)$ of atoms and segments in DMPC molecules and $\rho_{\rm w}(z)$ for each system. Black lines indicate $\rho(z)$ of atoms and segments in surfactant molecules. Note that in panels D and E $\rho_{\rm w}(z)$ ends at the periodic boundary along the z axis. The errors defined as the standard deviation values among five 10 ns interval averages are less than line thickness.

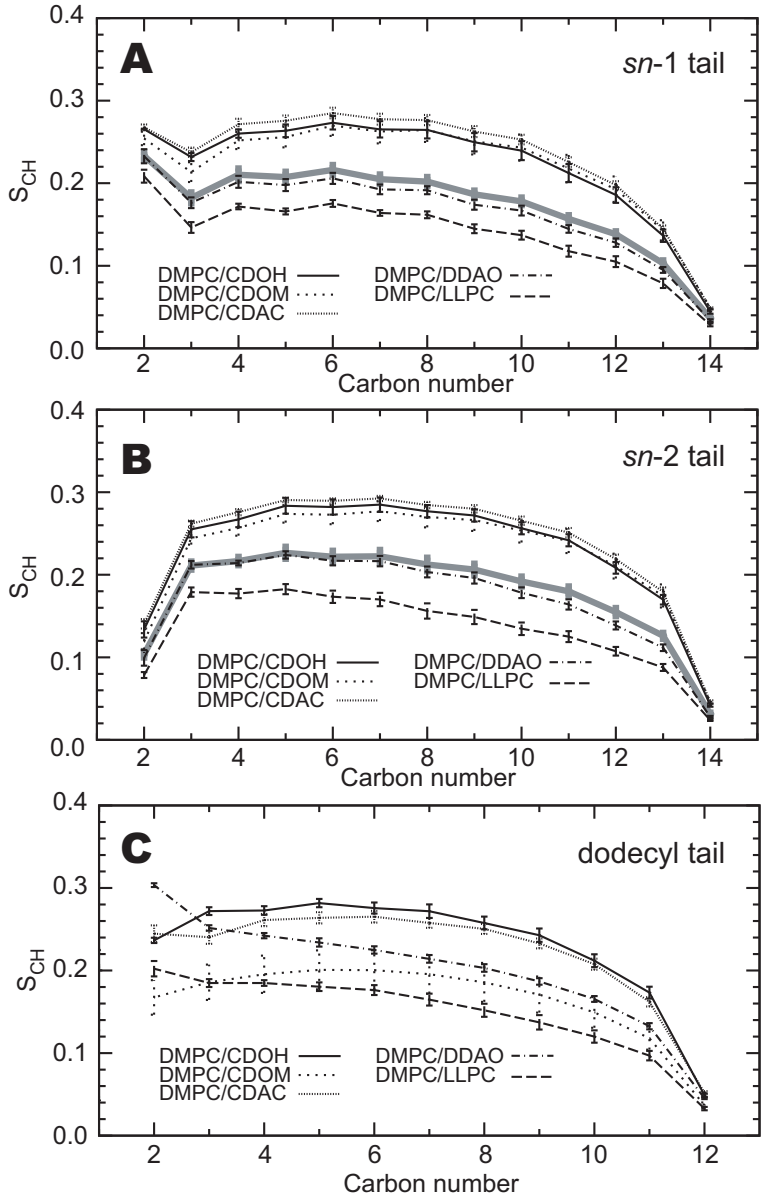

Figure 3: The calculated order parameter of the C–H vector in the *sn*-1 and *sn*-2 acyl tails of a DMPC molecule (panels A and B) and dodecyl tail of a surfactant molecule (panel C). In panels A and B, S_{CH} in pure DMPC bilayers, under the same thermodynamics conditions [12], is depicted here as a reference (thick gray line). The number of carbon atoms is the same as in Fig. 1. The error bars are the standard deviation values among five 10 ns interval averages.

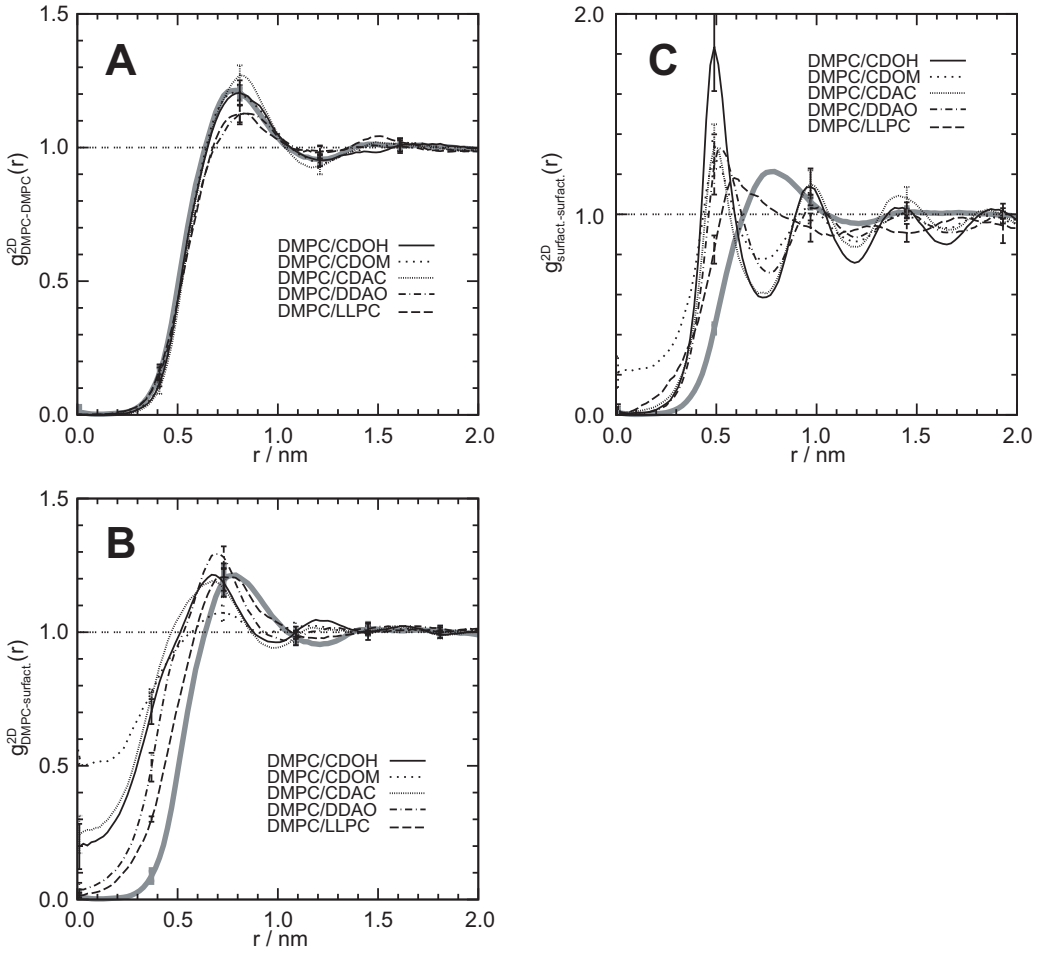

Figure 4: The calculated 2D radial distribution function between centers of mass for lipid molecules. Panel A: between DMPC–DMPC molecules, $g^{\mathrm{2D}}_{\mathrm{DMPC-DMPC}}(r)$; Panel B: between DMPC–surfactant molecules, $g^{\mathrm{2D}}_{\mathrm{DMPC-surfact.}}(r)$; Panel C: between surfactant–surfactant molecules, $g^{\mathrm{2D}}_{\mathrm{surfact.-surfact.}}(r)$. As a reference, $g^{\mathrm{2D}}_{\mathrm{DMPC-DMPC}}(r)$ in pure DMPC bilayers, under the same thermodynamic conditions [12], is depicted here in each panel (thick gray line). The error bars are the standard deviation values among five 10 ns interval averages.

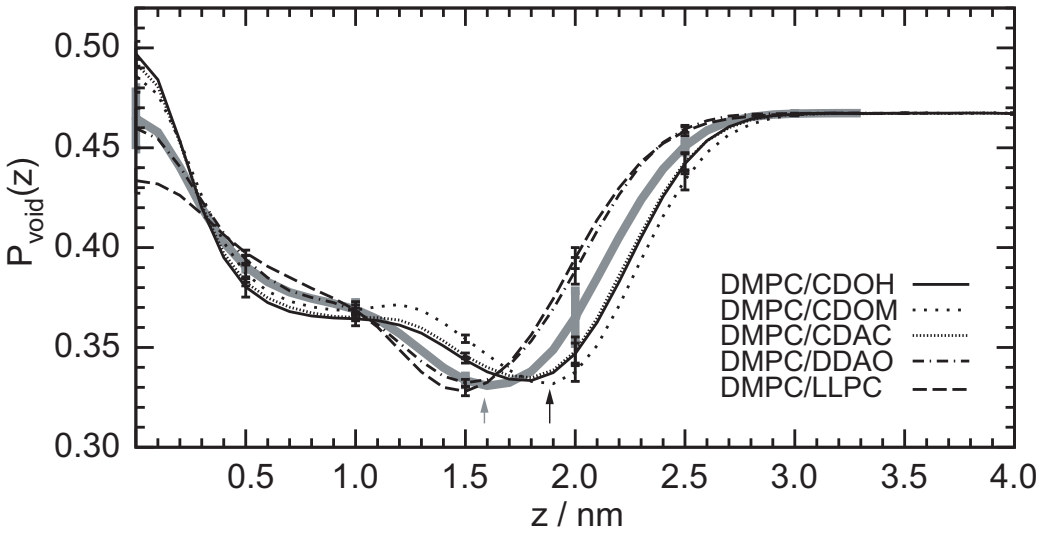

Figure 5: The calculated probability distribution of voids along the z axis, $P_{\rm void}(z)$. As a reference, $P_{\rm void}(z)$ in pure DMPC bilayers, under the same thermodynamic conditions [12], is depicted (thick gray line). Two upward small arrows indicate the position of minima of $P_{\rm void}(z)$ for a DMPC/CDOM bilayer (black arrows) and a pure DMPC bilayer (gray arrows). Scaled $P_{\rm void}(z)$ for DMPC/CDOM and DMPC/DDAO binary bilayers, compared with $P_{\rm void}(z)$ for a pure DMPC bilayer, are shown in Fig. S6 in the Supplementary Material. The error bars are the standard deviation values among five 10 ns interval averages.